3206 *Chem. Mater.* **2010,** *22,* 3206–3211
DOI:10.1021/cm100363a

CHEMISTRY OF MATERIALS
Article

Facile Fabrication of Honeycomb-Patterned Thin Films of Amorphous Calcium Carbonate and Mosaic Calcite

Cheng Li, Guosong Hong, Han Yu, and Limin Qi*

Beijing National Laboratory for Molecular Sciences (*BNLMS*), *State Key Laboratory for Structural Chemistry of Unstable and Stable Species, College of Chemistry, Peking University, Beijing 100871, People's Republic of China*

Received February 4, 2010. Revised Manuscript Received March 28, 2010

Facile fabrication of honeycomb-patterned thin films of amorphous calcium carbonate (ACC) and mosaic calcite was achieved via colloidal lithography at the solution surface. At first, honeycomb-patterned ACC (HP-ACC) thin films were fabricated by a polymer-induced ACC coating of the monolayer colloidal crystal (MCC) template at the air/water interface. Subsequent controlled crystallization of the preformed HP-ACC thin films under different conditions led to honeycomb-patterned, crystalline films with different microstructures. In particular, honeycomb-patterned, mosaic calcite thin films composed of single-crystalline calcite plates could form when thermal treatment at 400 °C was applied to the amorphous films. Additionally, dye molecules were incoporated into the HP-ACC thin film during its formation, enabling further functionality of the patterned thin film with fluorescence. Furthermore, the highly ordered HP-ACC thin films possessed brilliant structural colors and exhibited typical photonic properties.

Introduction

Two-dimensional (2D) patterned structures have attracted great interest of materials scientists due to their wide-range applications in optics, electronics, and sensing.[1−4] In particular, improved photonic functionalities including antireflection, structural color, and photonic band gap have been demonstrated by coating surfaces with 2D periodic structures with periodicities in the range of submicrometer length scale.[5−9] Specifically, spherical or hemispherical shell arrays have shown size-dependent diffraction properties due to their periodic modulation of the dielectric function, which can inhibit the propagation of certain frequencies of light through specific crystal orientations.[9−18] It may be noted that the spherical and hemispherical shell arrays exhibit quite different surface topographies, which may lead to considerable differences in optical and surface properties. To fabricate such highly ordered shell arrays with feature sizes down to the submicrometer length scale, patterning methods involving monolayer colloidal crystals (MCCs) as templates have been recognized to be a cost-efficient bottom-up strategy.[19] Usually, MCCs are composed of hexagonal-close-packed (hcp) colloidal spheres with uniform sizes ranging from a few hundred nanometers to several micrometers. The highly ordered sphere arrays of the MCCs make them perfect replicable templates for the production of half-shell structures by coating their surfaces through either dry methods including physical deposition[11−16,18] or wet methods involving sol−gel chemistry[10] and electro- or electroless chemical deposition.[9,15,17] Until now, shell or half-shell arrays of various inorganic materials, including titania,[10] zinc oxide,[11] silicon,[12] gold,[13−16] silver,[17,18] and $Ni(OH)_2$[9] have been fabricated with most of them associated with interesting anomalous optical properties. However, the development of mild, facile, and low-cost

*To whom correspondence should be addressed. E-mail: liminqi@pku.edu.cn. Fax: +86-10-62751708.

(1) Henzie, J.; Barton, J. E.; Stender, C. L.; Odom, T. W. *Acc. Chem. Res.* **2006**, *39*, 249.
(2) Park, S.; Xiong, Y.; Kim, R.; Elvikis, P.; Meitl, M.; Kim, D.; Wu, J.; Yoon, J.; Yu, C.; Liu, Z.; Huang, Y.; Hwang, K.; Ferreira, P.; Li, X.; Choquette, K.; Rogers, J. A. *Science* **2009**, *325*, 977.
(3) Anker, J. N.; Hall, W. P.; Lyandres, O.; Shah, N. C.; Zhao, J.; Van Duyne, R. P. *Nat. Mater.* **2008**, *7*, 442.
(4) Camden, J. P.; Dieringer, J. A.; Zhao, J.; Van Duyne, R. P. *Acc. Chem. Res.* **2008**, *41*, 1653.
(5) Min, W.; Jiang, B.; Jiang, P. *Adv. Mater.* **2008**, *20*, 3914.
(6) Zhu, J.; Yu, Z.; Burkhard, G. F.; Hsu, C.; Connor, S. T.; Xu, Y.; Wang, Q.; McGehee, M.; Fan, S.; Cui, Y. *Nano Lett.* **2009**, *9*, 279.
(7) Sato, O.; Kubo, S.; Gu, Z. *Acc. Chem. Res.* **2009**, *42*, 1.
(8) Li, Y.; Zhang, J.; Zhu, S.; Dong, H.; Jia, F.; Wang, Z.; Sun, Z.; Zhang, L.; Li, Y.; Li, H.; Xu, W.; Yang, B. *Adv. Mater.* **2009**, *21*, 4731.
(9) Duan, G.; Cai, W.; Luo, Y.; Sun, F. *Adv. Funt. Mater.* **2007**, *17*, 644.
(10) Rengarajan, R.; Jiang, P.; Colvin, V.; Mittleman, D. *Appl. Phys. Lett.* **2000**, *77*, 3517.
(11) Gao, Y.; Li, A. D.; Gu, Z. B.; Wang, Q. J.; Zhang, Y.; Wu, D.; Chen, Y. F.; Ming, N. B.; Ouyang, S. X.; Yu, T. *Appl. Phys. Lett.* **2007**, *91*, 031910.
(12) Landstrom, L.; Brodoceanu, D.; Arnold, N.; Piglmayer, K.; Bauerle, D. *Appl. Phys. A: Mater. Sci. Process.* **2005**, *81*, 911.
(13) Baia, L.; Baia, M.; Popp, J.; Astilean, S. *J. Phys. Chem. B* **2006**, *110*, 23982.
(14) Zhan, P.; Wang, Z.; Dong, H.; Sun, J.; Wu, J.; Wang, H.; Zhu, S.; Ming, N.; Zi, J. *Adv. Mater.* **2006**, *18*, 1612.
(15) Dong, W.; Dong, H.; Wang, Z.; Zhan, P.; Yu, Z.; Zhao, X.; Zhu, Y.; Ming, N. *Adv. Mater.* **2006**, *18*, 755.
(16) Huang, W.; Qian, W.; El-Sayed, M. A. *Adv. Mater.* **2008**, *20*, 733.
(17) Chen, Z.; Zhan, P.; Wang, Z.; Zhang, J.; Zhang, W.; Ming, N.; Chan, C. T.; Sheng, P. *Adv. Mater.* **2004**, *16*, 417.
(18) Farcau, C.; Astilean, S. *J. Opt. A: Pure Appl. Opt.* **2007**, *9*, S345.
(19) Li, Y.; Cai, W.; Duan, G. *Chem. Mater.* **2008**, *20*, 615.

Published on Web 04/20/2010

solution approaches toward such microstructured films made of desirable materials still remains a challenge.

On the other hand, one inspiration from biomineralization for materials processing is to provide alternative approaches to the synthesis of ceramic thin films under mild conditions instead of otherwise high-vacuum or high-temperature processing.[20−24] Significantly, amorphous phase, such as amorphous calcium carbonate (ACC), can readily form thin film coatings on solid substrates induced by polymers with or without specific chemical environment on the solid surfaces.[25−33] This polymer-induced ACC coating process bears some similarity to the sol−gel processing of ceramics in molding and shaping of fluidic precursors, but the ACC thin films do not need to be densified by heat-treatment like the case for gel-derived ceramics.[34] Recently, increasing attention has been paid to the fabrication of patterned $CaCO_3$ thin films due to the importance of patterning for both scientific and industrial applications. Chemically micropatterned templates including self-assembled monolayers,[35−37] layer-by-layer films,[38] polymer films,[39] and polymer brushes[40] have been used for the selective deposition of ACC thin films and their subsequent crystallization. By now, several in vitro experiments have succeeded in molding ACC into intricate shapes using micro- or nanostructured templates by adopting this strategy,[41−46] such as the infiltration of polymeric colloidal crystals with ACC to obtain three-dimensionally ordered macroporous (3DOM) calcite single crystals.[45] However, there are rare reports on the molding and shaping ACC directly into large-area thin films with ordered patterns of submicrometer length scale.

Herein, we report on the facile fabrication of honeycomb-patterned calcium carbonate (HP-$CaCO_3$) thin films via polymer-induced ACC coating of MCCs at the air/water interface. Recently, we have shown that MCCs can be used as floating masks at the gas/solution interface to fabricate through-pored nanonet thin films of various inorganic materials.[47] In this paper, we demonstrate that the strategy of colloidal lithography at the solution surface can be extended to the production of honeycomb-patterned ACC (HP-ACC) and mosaic calcite (HP-calcite) thin films. The HP-ACC thin film can be functionalized with fluorescence by synchronous inclusion of water-soluble dyes during the film formation. Furthermore, transmissivity measurement of the HP-ACC thin film was carried out to reveal its photonic properties.

Experimental Section

Chemicals and Materials. Calcium chloride ($CaCl_2$, 99%, Alfa Aesar), ammonium carbonate ($(NH_4)_2CO_3$, $NH_3 \geq 40\%$, Beijing Chemical Co.), poly(acrylic acid, sodium salt) (PAA, $M_w = 5100$, Aldrich), and Rhodamine B (RB, Beijing Chemical Co.) were used as received. Polystyrene (PS) colloidal spheres with a diameter of 470 ± 10 nm were synthesized by the surfactant-free emulsion polymerization.[48]

ACC Coating of MCCs at the Air/Water Interface. First, a piece of MCC film with an area of 1 cm^2 that was deposited on a silicon substrate[49] was transferred onto the surface of the precursor solution containing 20 mM $CaCl_2$ and 80 mg/L PAA. The vessel holding both the precursor solution and the floating MCC film was covered with Parafilm punched with one small aperture and put inside a closed desiccator with 2 g of $(NH_4)_2CO_3$ powder located at its bottom. The coating process took place at 25 ± 1 °C and lasted for 6 h before the composite film was picked up with substrates such as glass plates, silicon plates, and TEM grids for certain characterization. The MCC template was then removed by dissolving the sample in dichloromethane to obtain intact HP-ACC thin films. In the case of dye inclusion, RB was additionally dissolved in the precursor solution to reach a concentration of 0.2 mM.

Crystallization of HP-ACC Thin Films. The as-obtained HP-ACC thin films were kept under three different conditions for crystallization: (i) at room temperature and a relative humidity (RH) 20−40%, (ii) at 80 °C and a constant RH of 90%, and (iii) a thermal treatment at 400 °C in air.

(20) Heuer, A. H.; Fink, D. J.; Laraia, V. J.; Arias, J. L.; Calvert, P. D.; Kendall, K.; Messing, G. L.; Blackwell, J.; Rieke, P. C.; Thompson, D. H.; Wheeler, A. P.; Veis, A.; Caplan, A. I. *Science* **1992**, *255*, 1098.
(21) Bunker, B. C.; Rieke, P. C.; Tarasevich, B. J.; Campbell, A. A.; Fryxell, G. E.; Graff, G. L.; Song, L.; Liu, J.; Virden, J. W.; McVay, G. L. *Science* **1994**, *264*, 48.
(22) Lange, F. F. *Science* **1996**, *273*, 903.
(23) Aksay, A.; Trau, M.; Manne, S.; Honma, I.; Yao, N.; Fenter, P.; Eisenberger, P. M. *Science* **1996**, *273*, 892.
(24) Gao, Y.; Koumoto, K. *Cryst. Growth Des.* **2005**, *5*, 1983.
(25) Xu, G.; Yao, N.; Aksay, I. A.; Groves, J. T. *J. Am. Chem. Soc.* **1998**, *120*, 11977.
(26) (a) Gower, L. A.; Tirrell, D. A. *J. Cryst. Growth* **1998**, *191*, 153. (b) Gower, L. B.; Odom, D. J. *J. Cryst. Growth* **2000**, *210*, 719.
(27) (a) Kato, K. *Adv. Mater.* **2000**, *12*, 1543. (b) Sugawara, A.; Ishii, T.; Kato, T. *Angew. Chem., Int. Ed.* **2003**, *42*, 5299.
(28) (a) Xu, X.; Han, J. T.; Cho, K. *Chem. Mater.* **2004**, *16*, 1740. (b) Han, J. T.; Xu, X.; Kim, D. H.; Cho, K. *Chem. Mater.* **2005**, *17*, 136. (c) Xu, X.; Han, J. T.; Kim, D. H.; Cho, K. *J. Phys. Chem. B* **2006**, *110*, 2764. (d) Han, J. T.; Xu, X.; Kim, D. H.; Cho., K. *Adv. Funct. Mater.* **2005**, *15*, 475.
(29) Volkmer, D.; Harms, M.; Gower, L.; Ziegler, A. *Angew. Chem., Int. Ed.* **2005**, *44*, 639.
(30) Miura, A.; Kotachi, A.; Oaki, Y.; Imai, H. *Cryst. Growth Des.* **2006**, *6*, 612.
(31) Sommerdijk, N. A. J. M.; van Leeuwen, E. N. M.; Vos, M. R. J.; Jansen, J. A. *CrystEngComm* **2007**, *9*, 1209.
(32) Oaki, Y.; Kajiyama, S.; Nishimura, T.; Imai, H.; Kato, T. *Adv. Mater.* **2008**, *20*, 3633.
(33) Hong, C.; Chu, C. *Langmuir* **2009**, *25*, 3045.
(34) Gower, L. B. *Chem. Rev.* **2008**, *108*, 4551.
(35) Aizenberg, J.; Black, A. J.; Whitesides, G. M. *J. Am. Chem. Soc.* **1999**, *121*, 4500.
(36) Kim, Y.-Y.; Douglas, E. P.; Gower, L. B. *Langmuir* **2007**, *23*, 4862.
(37) Han, T. Y.; Aizenberg, J. *Chem. Mater.* **2008**, *20*, 1064.
(38) Lu, C.; Qi, L.; Ma, J.; Cheng, H.; Zhang, M.; Cao, W. *Langmuir* **2004**, *20*, 7378.
(39) Popescu, D. C.; van Leeuwen, E. N. M.; Rossi, N. A. A.; Holder, S. J.; Jansen, J. A.; Sommerdijk, A. J. M. *Angew. Chem., Int. Ed.* **2006**, *45*, 1762.
(40) Tugulu, S.; Harms, M.; Fricke, M.; Volkmer, D.; Klok, H.-A. *Angew. Chem., Int. Ed.* **2006**, *45*, 7458.
(41) (a) Loste, E.; Meldrum, F. C. *Chem. Commun.* **2001**, 901. (b) Park, R. J.; Meldrum, F. C. *Adv. Mater.* **2002**, *14*, 1167. (c) Loste, E.; Park, R. J.; Warren, J.; Meldrum, F. C. *Adv. Funct. Mater.* **2004**, *14*, 1211.
(42) Aizenberg, J.; Muller, D. A.; Grazul, J. L. *Science* **2003**, *299*, 1206.
(43) Gehrke, N.; Nassif, N.; Pinna, N.; Antonietti, M.; Gupta, H. S.; Colfen, H. *Chem. Mater.* **2005**, *17*, 6514.
(44) Cheng, X.; Gower, L. B. *Biotechnol. Prog.* **2006**, *22*, 141.
(45) Li, C.; Qi, L. *Angew. Chem., Int. Ed.* **2008**, *47*, 2388.
(46) Finnemore, A. S.; Scherer, M. R. J.; Langford, R.; Mahajan, S.; Ludwigs, S.; Meldrum, F. C.; Steiner, U. *Adv. Mater.* **2009**, *21*, 3928.
(47) Li, C.; Hong, G.; Qi, L. *Chem. Mater.* **2010**, *22*, 476.
(48) Holland, B. T.; Blanford, C. F.; Do, T.; Stein, A. *Chem. Mater.* **1999**, *11*, 795.
(49) Li, C.; Hong, G.; Wang, P.; Yu, D.; Qi, L. *Chem. Mater.* **2009**, *21*, 891.

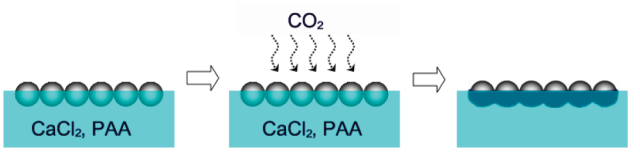

Figure 1. Schematic illustration of the fabrication of HP-$CaCO_3$ thin film by colloidal lithography at the solution surface.

Characterization. Microstructures of the samples were characterized by field-emission scanning electronic microscopy (SEM, Hitachi FE-S4800, 5 kV), transmission electronic microscopy (TEM, JEOL JEM 200CX, 160 kV), and selected area electron diffraction (SAED). Optical and fluorescence micrographs were taken with a Nikon ECLIPSE E600 fluorescence microscope equipped with polarizers. Powder X-ray diffraction (XRD) spectra were recorded on a Rigaku Dmax-2000 X-ray diffractometer with Cu Kα radiation. Infrared (IR) spectra were scanned at 1 cm^{-1} resolution with a Nicolet iNIO MX micro-FTIR instrument. Thermogravimetric analysis (TGA) was performed by heating the films at 10 °C min^{-1} in a flow of air with a SDT2960 thermogravimetric analyzer (Thermal Analysis). The transmission spectra were obtained on a Hitachi U-4100 spectrophotometer with normal incidence.

Results and Discussion

Figure 1 schematically shows the fabrication of HP-$CaCO_3$ thin films by colloidal lithography at the solution surface. After mineralization for 6 h, the PS-ACC composite film was picked up from the solution surface with a solid substrate. Figure 2a shows a typical SEM image of the as-obtained PS-ACC composite film, where the PS MCC template was embedded in a uniform film. After removal of the template, hollow half-shell thin films composed of hemispherical chambers with a diameter of 450 nm were obtained (Figure 2b). Figure 2c displays a perspective SEM view of the patterned thin film, suggesting a film thickness of about 600 nm. It also shows that the hcp-arranged chambers are interconnected with each other through small windows on the chamber walls, resulting from the dense packing of the pristine MCC template. Figure 2d shows its reverse side (i.e., the side facing the subphase during the ACC coating), indicating that the ACC coating consists of amalgamated particles with diameters in the range of 80−100 nm. Overall, the coating layer inherited the basic profile of the MCC template, resulting in the honeycomb-patterned thin films of connected hollow half-shell arrays in a large area.

To investigate the ACC coating process, we observed the thin films obtained at different periods of reaction with SEM (Figure S1, Supporting Information). Initially, ACC particles were deposited at the interstices of the MCC template at the solution surface, resulting in the formation of a through-pored net-like film, as reported previously.[41] Further deposition of ACC occurred at the reverse side of the MCC template underneath the solution until it was completely coated after 6 h of reaction (Figure 2d). The sequence of the ACC deposition can be attributed to the priority of accessibility to the diffusive CO_2 gas. The solution surface between the PS colloidal spheres was more accessible by CO_2 than the bulk solution.

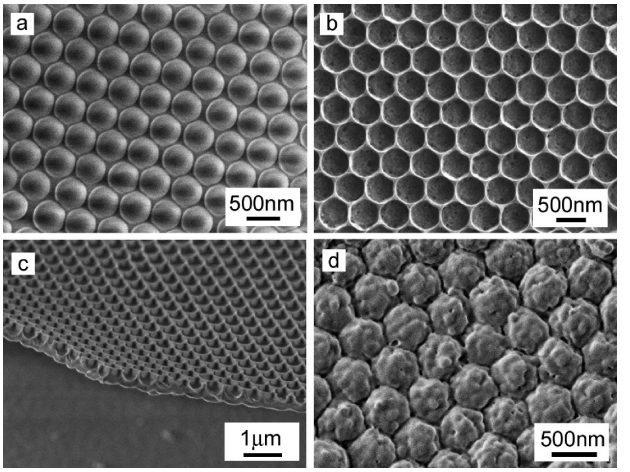

Figure 2. SEM images of (a) PS-ACC composite film and (b−d) HP-ACC thin film after template removal: (b) top view, (c) lateral view, and (d) bottom view.

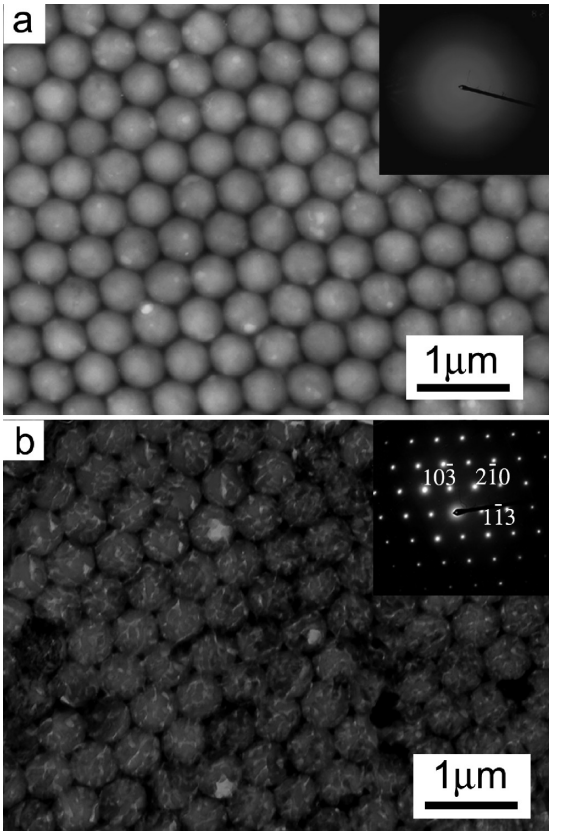

Figure 3. TEM images of amorphous (a) and crystalline (b) HP-$CaCO_3$ films. Insets show the corresponding SAED patterns.

Once the solution surfaces between the PS colloidal spheres were stuffed with the ACC particles, the diffusive gas was blocked from this pathway and could only diffuse into the bulk solution through the bare solution surface without the PS sphere monolayer. Meanwhile, the heterogeneous deposition or coating of the underwater surfaces of PS colloidal spheres by ACC was initiated by the CO_3^{2-} anion dissociated from dissolved CO_2.

To reveal the composition and microstructure of the as-obtained HP-$CaCO_3$ thin film, characterizations by TEM, IR, and TG analysis were performed. Figure 3a

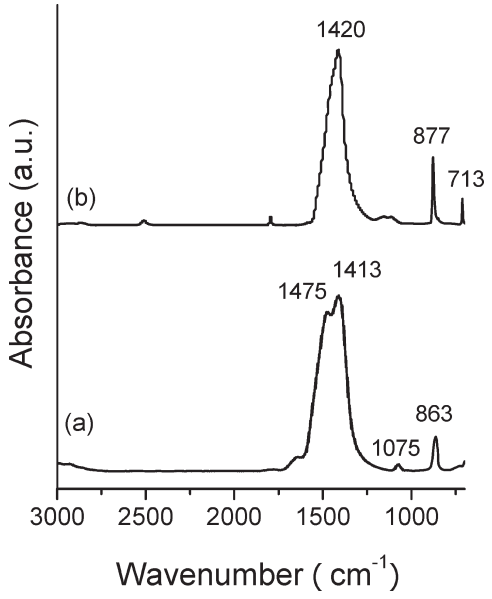

Figure 4. IR spectra of amorphous (a) and crystalline (b) HP-$CaCO_3$ thin films.

shows a typical TEM image of the HP-$CaCO_3$ thin film together with the corresponding SAED pattern. The film exhibited regular hexagonal patterns and rather smooth textures. The diffusive rings of the SAED pattern suggest that the thin film was amorphous. The IR spectrum of the thin film shows ν_2 (out of plane bending) peak at 863 cm^{-1}, split ν_3 (asymmetric stretch) peaks at 1413 cm^{-1} and 1475 cm^{-1}, and an additional broad ν_1 (asymmetric stretch) peak around 1075 cm^{-1} (Figure 4a), which are characteristic of ACC.[50] The absence of ν_4 (in-plane bending) peak at 713 cm^{-1} indicates that well-ordered calcite is not present.[50] These results indicate that the as-obtained HP-$CaCO_3$ thin film was composed of ACC. The TG curve of the HP-ACC thin film shows a three-step weight loss (Figure S2, Supporting Information). The weight loss below 300 °C can be attributed to the dehydration process. The weight loss around 500 °C can be attributed to the burning off of the organic species PAA. The PAA content was estimated to be about 0.9 wt %, which means that a small amount of PAA was included during the ACC coating process. $CaCO_3$ started to decompose at 700 °C, corresponding to the third weight loss in the TG curve. These results suggested that the coating of MCC template occurred through a polymer-induced ACC formation process, which has been widely reported in the $CaCO_3$ mineralzation.[25−33]

The transformation of HP-ACC thin films into crystalline calcite thin films can be achieved three different ways. In the first way, the HP-ACC thin film was kept under ambient conditions, that is, at room temperature and a relative humidity around 20−40%. In this case, the crystallization process was rather slow, and it took around 7 days for the amorphous film to crystallize completely. As shown in Figure 5a, the film cracked into small pieces due to drying. The corresponding polarized

(50) Aizenberg, J.; Lambert, G.; Addadi, L.; Weiner, S. *Adv. Mater.* **1996**, *8*, 222.

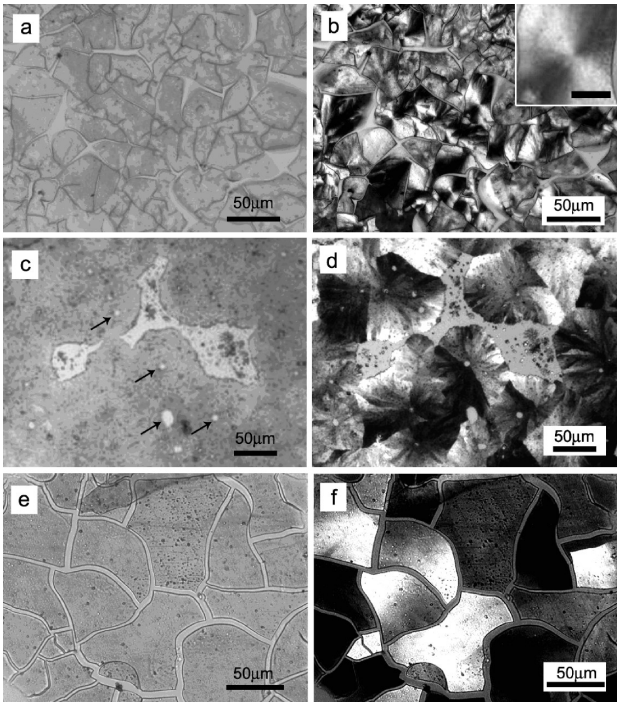

Figure 5. Optical micrographs of crystalline HP-$CaCO_3$ thin films obtained under three different conditions: (a, b) room temperature and 20−40% RH, (c, d) 80 °C and 90% RH, and (e, f) 400 °C. (a, c, e) are micrographs taken under normal light, and (b, d, f) are the corresponding polarized optical micrographs. Inset: high-magnification image illustrating the texture of a spherulitic domain (scale bar: 10 μm).

optical micrograph shown in Figure 5b revealed that the honeycomb-patterned thin film was spherulitic and polycrystalline, which is in accordance with the formation of flat polycrystalline spherulitic $CaCO_3$ films under similar crystallization conditions.[28] In the second way, the amorphous HP-ACC thin film was subjected to a high RH (90%) and a relative high temperature (80 °C), which could accelerate the crystallization process. Under this condition, the time needed for complete crystallization could be shortened to 2 days. From the optical micrograph in Figure 5c, we can see that the film did not split probably due to the high RH applied. However, large-area land of void formed in the continuous film after crystallization. Besides, many smaller voids also appeared, as indicated by the black arrows in Figure 5c. The corresponding polarized optical micrograph shows clearly large-area spherulitic domains (Figure 5d). These results suggest that the amorphous phase underwent a dissolution−recrystallization process, which was probably induced by the high RH. In the last approach, a very high temperature was applied to enhance the crystallization process of the amorphous phase. This was achieved by heating the amorphous thin film at 400 °C for 2 h in air. After the thermal treatment, the film cracked into relatively large pieces, as can be seen from the optical micrograph in Figure 5e. However, what is unusual is that the thin film had turned into a mosaic film of single-crystal plates, and these single-crystal plates disconnected themselves with each other, which was confirmed by the polarized optical micrograph shown in Figure 5f. The single-crystalline plates in the film can reach an area of up

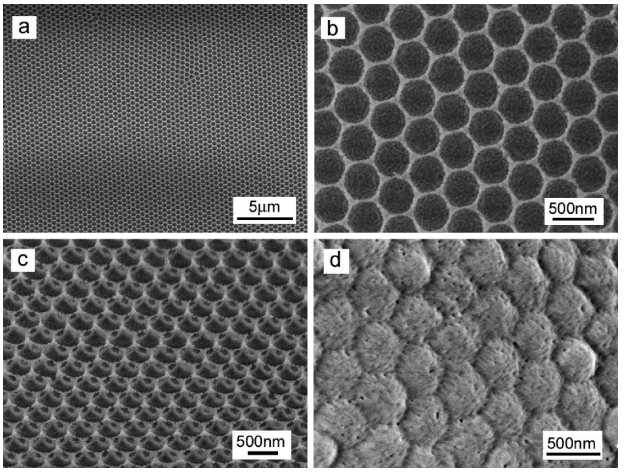

Figure 6. SEM images of crystalline HP-$CaCO_3$ thin film after heat treatment at 400 °C for 2 h: (a, b) top view, (c) tilted view, and (d) bottom view.

to 5×10^3 μm^2, which was estimated to contain $\sim 2 \times 10^4$ half-shells. The disconnection between the single-crystal plates was probably caused by the tension arising from the volume shrinkage during each single nucleation and crystallization event.

The mosaic crystalline thin film was characterized by SEM, TEM, FT-IR, and XRD to reveal the morphology and microstructure of the single-crystalline plates within the crystalline film. Figure 6a,b shows the low and high magnification SEM images of a single plate, respectively. As can be seen, large-area, highly ordered hollow half-shell arrays were well retained in the crystalline film, and the orderly arranged chambers had an identical diameter around 450 nm. More details of the geometry of the crystalline film can be found in a topographic image shown in Figure 6c, which clearly reveals that the chambers were interconnected with each other via the small holes formed in the chamber walls because of the close packing of the template spheres. The reverse side of the crystalline film was still made up of arrays of half-shell (Figure 6d). However, in contrast to the amorphous film shown in Figure 2d, the surface texture of the crystalline film apparently changed. Numerous tiny pores and interstices formed, which was consistent with the TEM image shown in Figure 3b. It also suggests that the sizes of the pores and interstices were about 20−50 nm. These pores and interstices were probably caused by the release of impurities and water during crystallization. The corresponding SAED pattern shows a regular array of sharp spots ascribed to the [361] zone axis of calcite, confirming that each plate was a single crystal (Figure 3b). The FT-IR spectrum of the as-obtained calcite thin film is shown in Figure 4b, which shows distinguished absorbent peaks at 1420 cm^{-1}, 877 cm^{-1}, and 713 cm^{-1}, corresponding to the ν_3, ν_2, and ν_4 peaks of calcite, respectively.[41] The related XRD pattern confirms that the crystalline phase was made of pure calcite (Figure S3, Supporting Information). The prominent (104) peak of calcite in the XRD pattern suggests the thin film was roughly (104) oriented. As far as we know, this is the first demonstration

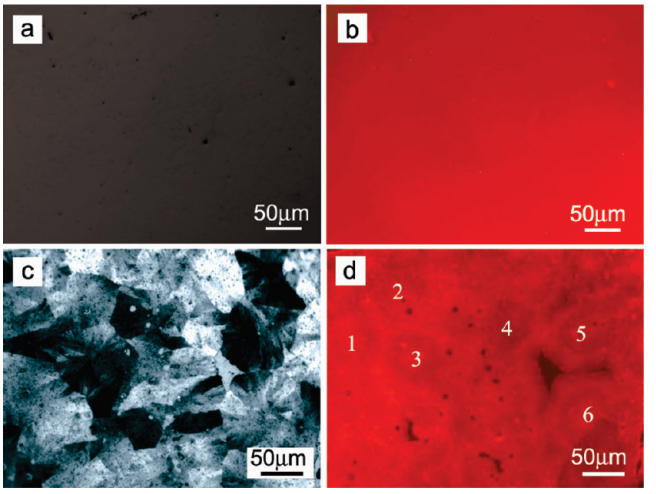

Figure 7. Optical micrographs of amorphous (a, b) and crystalline (c, d) HP-$CaCO_3$ thin films with the dye RB included. Crystallization was conducted at 80 °C and 90% RH. (a, c) are polarized optical micrographs, and (b, d) are the corresponding fluorescent micrographs.

of highly oriented mosaic single-crystal calcite films with highly ordered, submicrometer-sized honeycomb patterns.

Furthermore, the HP-ACC thin film was functionalized with fluorescence by synchronous inclusion of water-soluble dyes during the mineral formation process, which could be realized thanks to the tolerance of ACC with impurities and water. For example, Kato et al. demonstrated the preparation of ACC-polymer composites.[32] Here we used Rhodamine B (RB) as the dopant dye by dissolving it in the precursor solution of $CaCl_2$ and PAA. The deposition of the ACC film onto the floating MCC template in the presence of RB was conducted by a similar experimental procedure. After removing the MCC template, the resulting RB-included HP-ACC thin film was soaked in water to get rid of the absorbed RB molecules. It may be noted that the RB-included HP-ACC thin film could also be prepared by dipping the prefabricated ACC thin film into the dye solution; however, the synchronous inclusion of the dye molecules during the mineralization enabled more uniform inclusion of the dye molecules within the amorphous film. Figure 7a shows the polarized optical micrograph of the as-obtained dye-included HP-ACC thin film. Its amorphous nature was confirmed by the complete darkness under polarized light. Figure 7b shows the corresponding fluorescent micrograph, which exhibited uniform red emission, suggesting that the dye molecules were included and dispersed homogenously in the ACC film.[32,51] Then, crystallization of the amorphous films with RB included was performed at 80 °C and 90% RH. Figure 7c shows the polarized optical micrograph of the crystallized HP-$CaCO_3$ thin film, which suggests that the film was made of large spherulitic domains, similar to the HP-$CaCO_3$ film obtained without dyes (Figure 5d). Figure 7d shows the corresponding fluorescence micrograph, which

(51) Sindhu, S.; Jegadesan, S.; Hairong, L.; Ajikumar, P. K.; Vetrichelvan, M.; Valiyaveettil, S. *Adv. Funct. Mater.* **2007**, *17*, 1698.

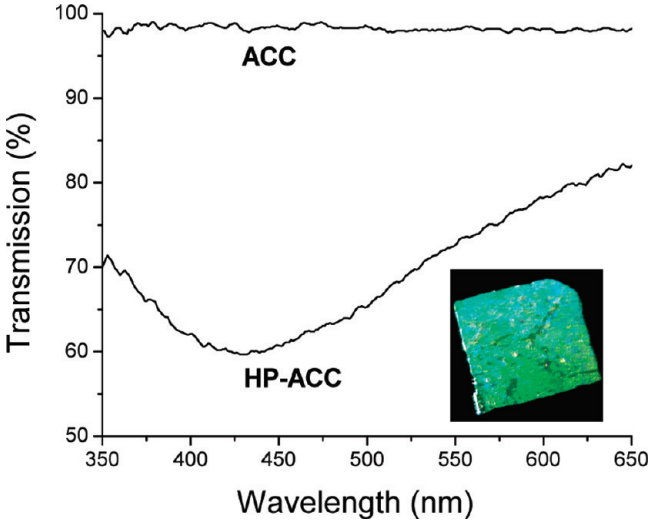

Figure 8. Transmission spectra of normal ACC and HP-ACC thin films. Inset is the photograph of HP-ACC thin film deposited on a silicon substrate ~ 1 cm^2.

exhibits round areas encircled by rings with stronger red emission, as indicated by the numbers in Figure 7d. The encircled round areas just corresponded to those spherulite domains, which suggest that dye molecules were excluded as impurity during the crystallization processes of ACC.[42] The protocol presented here might enable us to observe the exclusion of impurities directly during crystallization provided in situ characterization could be used.

The periodic submicrometer-sized air voids of the HP-$CaCO_3$ thin film led to strong diffraction of visible light and therefore intense structural colors. Figure 8 shows a representative photograph of a piece of HP-ACC thin film on Si substrate ~1 cm^2 in area, which exhibited a brilliant green color. In contrast, the normal ACC thin film obtained at the bare solution surface without the MCC template (Figure S4, Supporting Information) was transparent and colorless, which was consistent with its structureless transmission spectrum (Figure 8). The transmission spectrum of the HP-ACC film showed a major minimum centered at 433 nm (Figure 8), which could be ascribed to the Rayleigh-Wood anomaly associated with diffraction due to 2D periodic structures.[11,12] These results indicated that the as-obtained HP-ACC film could act as a photonic material with structural colors brought about by its periodic structure. It is expected the crystalline HP-calcite thin film might have interesting photonic properties due to its anisotropic refractive index. Unfortunately, we have been unable to attain reliable spectra of the mosaic HP-calcite film so far because of the poor integrity of the crystalline thin films due to cracking upon crystallization. Further efforts are under way to realize the crystallization of the HP-ACC thin film without significant cracking.

Conclusions

In conclusion, we have demonstrated the facile fabrication of HP-$CaCO_3$ thin films via colloidal lithography at the solution surface. Large-area HP-ACC thin films consisting of highly ordered submicrometer hollow half-shell arrays were produced via polymer-induced ACC coating of MCC templates floating at the air−water interface. Honeycomb-patterned, mosaic calcite thin films consisting of single-crystalline domains about tens of micrometers in size were obtained by controlled crystallization of the HP-ACC thin films. The floating template at the air−water interface in combination with the gas diffusion method provides a facile templating route for the shaping and molding of amorphous calcium carbonate thin film. The controlled crystallization of amorphous phase with retained shapes and patterns represents an alternative route to patterned crystalline thin films. The highly ordered HP-$CaCO_3$ thin film demonstrates interesting structural colors. Moreover, the versatility of this method enables the simultaneous inclusion of functional molecules into the amorphous thin films, endowing the patterned thin films with further functions that may find applications in biological and optoelectronics. Furthermore, the honeycomb structures presented by such films and the good biocompatibility of $CaCO_3$ may make such films promising candidates for 2D scaffolds for cell culture such as bone cell culture.[52]

Acknowledgment. Financial support from NSFC (Grants 20873002, 20633010, and 50821061), MOST (Grant 2007CB936201), and SRFDP (Grant 20070001018) is gratefully acknowledged.

Supporting Information Available: Additional characterizations of the thin films of HP-ACC, HP-calcite, RB included HP-ACC, and normal ACC (PDF). This material is available free of charge via the Internet at http://pubs.acs.org.

(52) Firkowska, I.; Godehardt, E.; Giersig, M. *Adv. Funct. Mater.* **2008**, *18*, 3765.